SUPPLEMENTARY INFORMATION

Full Antagonism of the Estrogen Receptor without a Prototypical Ligand Side Chain

Sathish Srinivasan[1a], Jerome C. Nwachukwu[1a], Nelson E. Bruno[1], Venkatasubramanian Dharmarajan[2], Devrishi Goswami[2], Irida Kastrati[3], Scott Novick[2], Jason Nowak[1], Valerie Cavett[1], Hai-Bing Zhou[4], Nittaya Boonmuen[5], Yuechao Zhao[5], Jian Min[6], Jonna Frasor[3], Benita S. Katzenellenbogen[5], Patrick R. Griffin[2], John A. Katzenellenbogen[6], Kendall W. Nettles[1]*

[1]Department of Cancer Biology, The Scripps Research Institute, 130 Scripps Way, Jupiter, Florida, 33458 USA

[2]Department of Molecular Therapeutics, The Scripps Research Institute, Jupiter, Florida, 33458 USA

[3]Department of Physiology and Biophysics, University of Illinois, 835 South Wolcott Avenue, Chicago, IL 60612 USA

[4] Key Laboratory of Combinatorial Biosynthesis and Drug Discovery (Wuhan University), Ministry of Education, State Key Laboratory of Virology, Wuhan University School of Pharmaceutical Sciences, Wuhan, 430071, China

[5]Department of Molecular and Integrative Physiology, University of Illinois, 407 South Goodwin Avenue, Urbana, IL 61801 USA

[6]Department of Chemistry, University of Illinois, 600 South Mathews Avenue, Urbana, Illinois, 61801 USA

[a]Contributed equally

*Corresponding author: Kendall W. Nettles

Email: knettles@scripps.edu

Supplementary Results

Supplementary Table 1. Data collection and refinement statistics (molecular replacement)

	1 (5KCC)	**4** (5KCD)	**5** (5KCE)	**7** (5KCF)
Data collection				
Space group	P 1 21 1	P 1 21 1	P 1 21 1	P 1 21 1
Cell dimensions				
a, *b*, *c* (Å)	54.53, 81.16, 58.68	55.95, 83.46, 58.78	52.58, 75.33, 58.00	54.88, 81.57, 58.90
α, β, γ (°)	90.00, 110.8, 90.00	90.00, 109.38, 90.00	90.00, 110.82, 90.00	90.00, 110.19, 90.00
Resolution (Å)	2.38 (2.42 – 2.38)*	1.82 (1.85 – 1.82)	1.85 (1.88 – 1.85)	2.07 (2.11 – 2.07)
R_{merge}	0.146 (0.865)	0.04 (0.299)	0.104 (0.81)	0.088 (0.84)
$I / \sigma I$	17.93 (1.79)	24.78 (5.68)	13.53 (1.93)	10.82 (2.03)
Completeness (%)	97.4 (99.5)	99.79 (99.96)	96.50 (95.19)	98.23 (98.09)
Redundancy	6.5 (6.7)	3.8 (3.8)	6.5 (6.0)	6.8 (6.5)
Refinement				
Resolution (Å)	2.4	1.8	1.8	2.1
No. reflections	17,204	45,612	35,066	29,350
R_{work} / R_{free}	0.2209 / 0.2623	0.1780 / 0.2062	0.1926 / 0.2493	0.1922 / 0.2347
No. atoms	3,894	4,205	4,023	4,031
Protein	3,730	3,826	3,760	3,783
Ligand/ion	62	64	99	63
Water	102	315	164	185
B-factors				
Protein	41.1	40.7	39.4	41.4
Ligand/ion	33.7	30.7	35.2	29.2
Water	36.6	45.5	41.7	39.2
R.m.s. deviations				
Bond lengths (Å)	0.009	0.01	0.009	0.006
Bond angles (°)	0.91	1.16	1.02	0.75

*1 crystal per structure. *Highest-resolution shell is shown in parentheses.

Supplementary Table 1 (continued)

	9 (5KCT)	**10** (5KCU)	**11** (5KCW)	**13** (5KD9)
Data collection				
Space group	P 1 21 1	P 1 21 1	P 1 21 1	P 1 21 1
Cell dimensions				
a, *b*, *c* (Å)	54.87, 81.56, 58.91	55.48, 82.22, 58.83	55.63, 81.53, 58.98	54.95, 81.65, 58.80
α, β, γ (°)	90.00, 110.18, 90.00	90.00, 110.83, 90.00	90.00, 110.93, 90.00	90.00, 110.97, 90.00
Resolution (Å)	1.60 (1.63 – 1.60)	2.03 (2.07 – 2.03)	1.90 (1.93 – 1.90)	1.78 (1.81 - 1.78)
R_{merge}	0.062 (0.728)	0.074 (0.734)	0.064 (0.71)	0.049 (0.674)
I / σI	19.09 (2.33)	14.91 (2.51)	18.49 (2.16)	18.13 (2.34)
Completeness (%)	96.61 (95.37)	98.26 (96.94)	97.02 (97.33)	97.08 (93.75)
Redundancy	6.7 (6.9)	6.8 (6.2)	6.7 (6.6)	6.9 (6.0)
Refinement				
Resolution (Å)	1.6	2.0	1.9	1.8
No. of reflections	62,295	31,413	37,369	45,180
R_{work} / R_{free}	0.1841 / 0.2135	0.1939 / 0.2497	0.1986 / 0.2449	0.1847 / 0.2142
No. atoms	4,306	3,880	3,962	4,070
Protein	3,877	3,707	3,724	3,829
Ligand/ion	68	74	99	62
Water	361	99	139	179
B-factors				
Protein	35.9	61.5	57	52.3
Ligand/ion	29.5	61.3	47.5	41.4
Water	43.4	47.3	51.3	47.4
R.m.s. deviations				
Bond lengths (Å)	0.008	0.006	0.011	0.008
Bond angles (°)	1.13	0.83	1.21	0.94

*1 crystal per structure. *Highest-resolution shell is shown in parentheses.

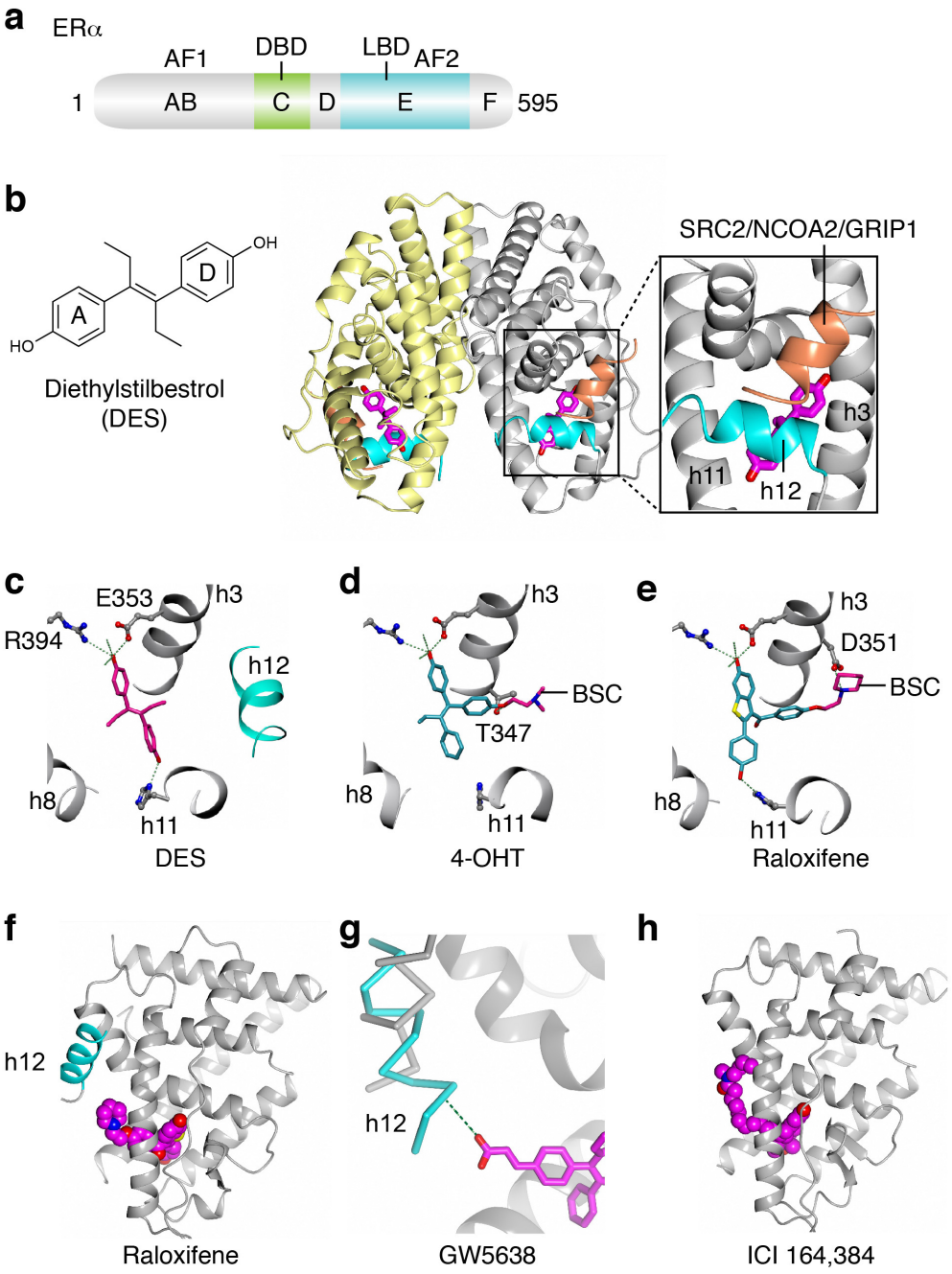

Supplementary Figure 1. Structural features of the ERα ligand-binding domain

(**a**) Schematic illustration of the ERα functional domains, A through F. The transcription activation functions, AF1 and AF2, the DNA-binding domain (DBD), and the ligand-binding domain (LBD) are indicated.

(**b**) Structure of the active ERα LBD dimer in complex with diethylstilbestrol (DES). In the active LBD conformation, the switch helix, h12, docks across h11 and h3 to form one side of the AF2 surface where the SRC2/NCOA2/GRIP1 peptide binds. (PDB 3ERD) [1]

(**c**–**e**) Structures of the ERα LBD showing the binding orientations of DES, and the SERMs 4-hydroxytamoxifen (4-OHT) and raloxifene (Ral) (PDBs 3ERD, 3ERT, 1ERR) [1,2].

(**f–g**) Structures of the inactive ERα LBD in complex with raloxifene or GW5638. (PDBs 1ERR, 1R5K)[2,3]

(**h**) Structure of the rat ERβ LBD in complex with a fulvestrant analog, ICI 164,384, showing the orientation of long hydrophobic side chain (PBD 1HJ1) [4].

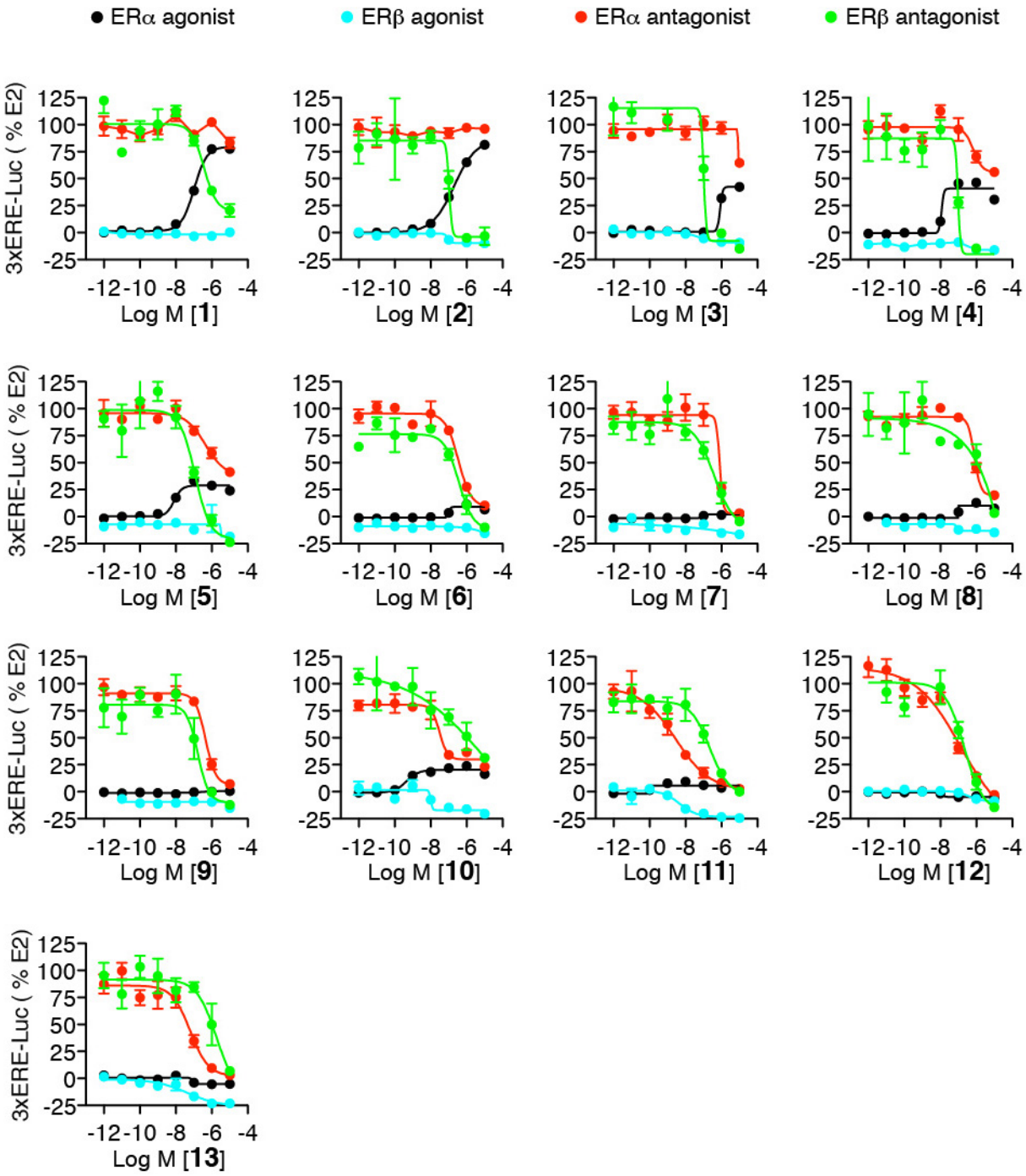

Supplementary Figure 2. Luciferase activity profiles of OBHS-N compounds in HepG2 cells for ERα and ERβ

HepG2 cells were transfected with 3xERE-luc and ERα or ERβ expression plasmids. The next day, cells were treated for 24 hr with dose curves of OBHS-N compounds **1**–**13** for the agonist assay and with 10 nM E2 for the antagonist assay. Data is shown as mean ± s.e.m. (n = 3). EC_{50} and IC_{50} values for these compounds have been reported earlier[8].

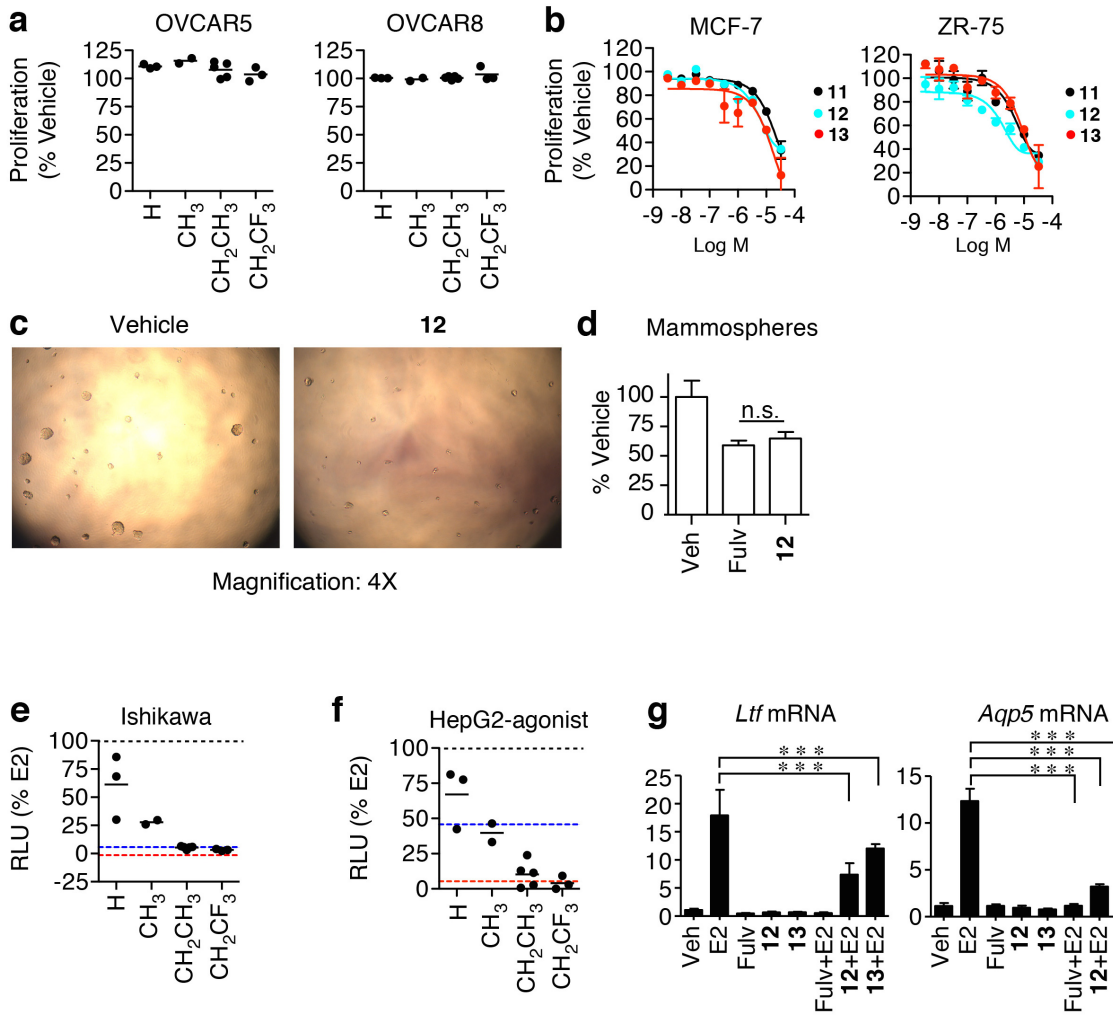

Supplementary Figure 3. Effects of OBHS-N analogs

(**a**) OVCAR5 and OVCAR8 cell lines were plated in phenol red free media and treated with 10 μM of the OBHS-N compounds on days 1 and 4. Cell number was calculated on day 7. $n = 3$ biological replicates.

(**b**) MCF-7 cells were plated in phenol red-free media and treated with the indicated compounds on days 1 and 4. Cell number was calculated on day 7. $n = 3$ biological replicates. Data is shown as mean ± s.e.m.

(**c–d**) MCF-7 cells were grown on low attachment plates and treated with 1 μM fulvestrant or 10 μM **12** and the number of spheres ≥ 75μm in diameter was determined.

(**e–f**) Luciferase assays. HepG2 cells were co-transfected with 3xERE-luc reporter and ERα-WT expression plasmids and Ishikawa cells were transfected with the reporter. Cells were steroid-deprived and treated with 10 μM OBHS-N ligands. Values are mean, $n = 3$.

(**g**) Uteri ($n = 4$ per group) from animals were analyzed for gene expression following treatment described in **Fig. 3h** and online methods. Values are mean ± s.e.m. Statistical significance was determined by ANOVA and Dunnett's Multiple Comparison test. *$p < 0.05$; **$p < 0.01$;***$p < 0.001$.

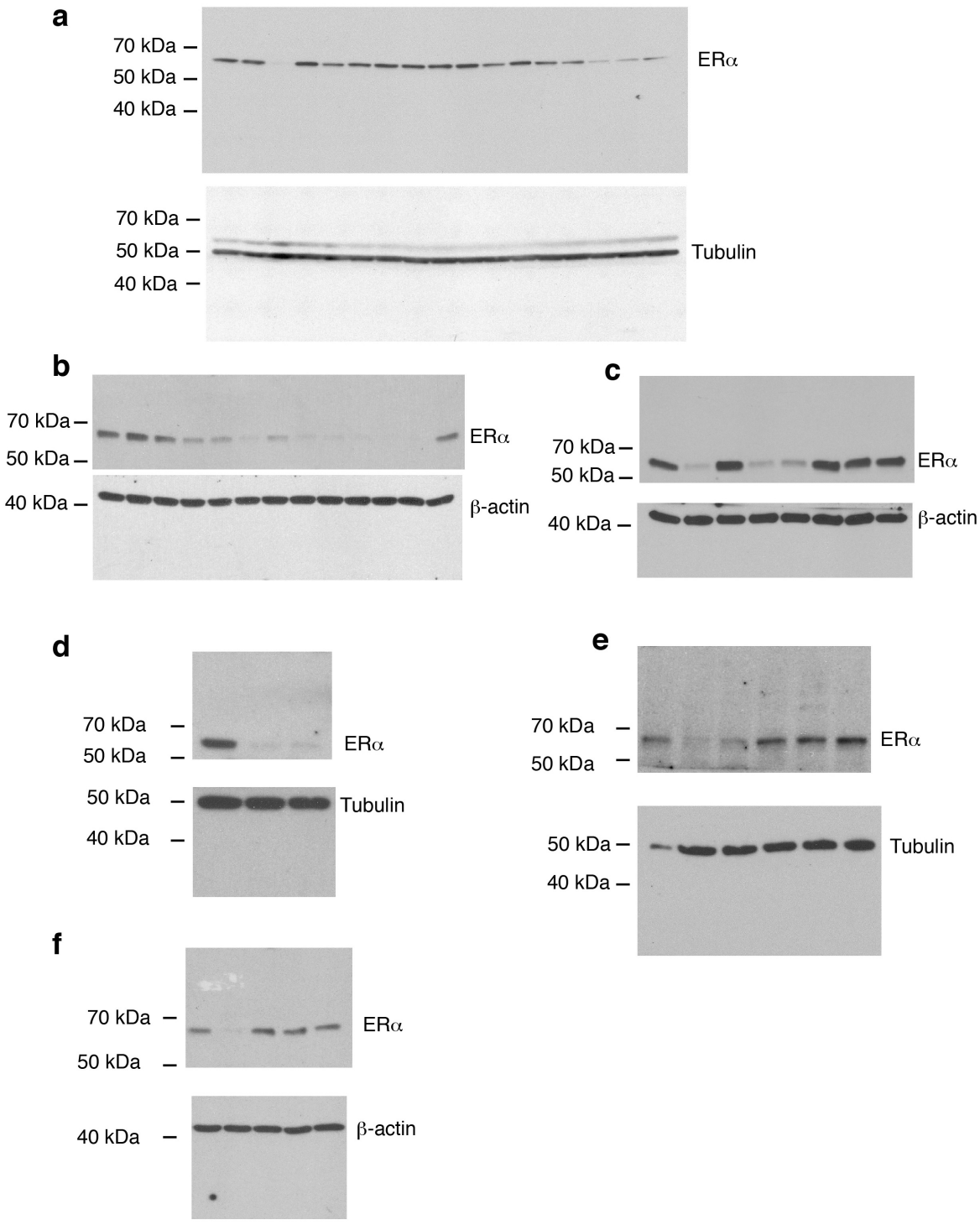

Supplementary Figure 4. Full gel images for western blots
(**a**) Figure 4a gel image
(**b**) Figure 4c gel image
(**c**) Figure 4e gel image
(**d**) Supplementary Figure 5a gel image
(**e**) Supplementary Figure 5b gel image
(**f**) Supplementary Figure 5c gel image

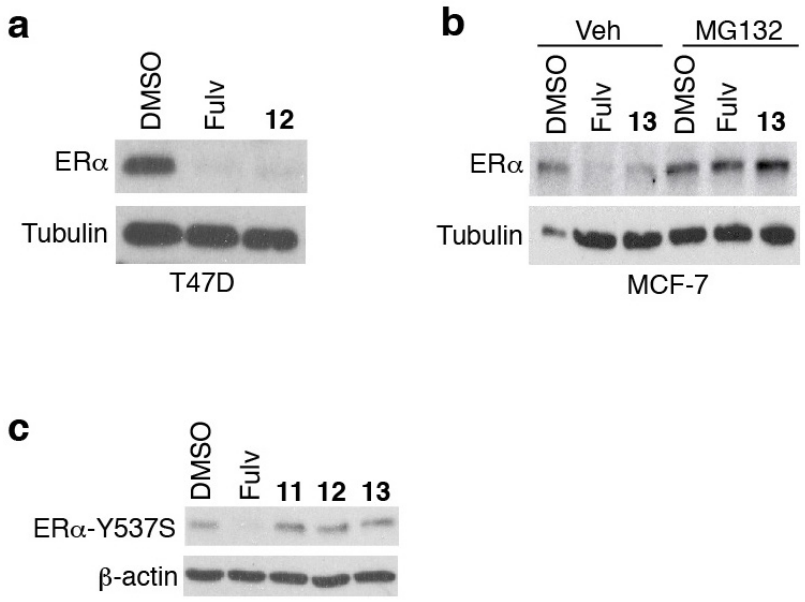

Supplementary Figure 5. Degradation of WT and Y537S ERα

(**a**) T47-D cells were treated with **12** (10 μM) or fulvestrant (10 nM) for 6 hr. Western blot was performed to detect ERα protein levels.

(**b**) MCF-7 cells were pre-treated with either vehicle or MG132 (10 μM) for 1 hr and then treated with **13** (10 μM) or fulvestrant (10 nM) for additional 6 hr. Western blot was performed to detect ERα protein levels.

(**c**) HeLa cells were transiently transfected with ERα-Y537S expression plasmid for 24 hr and then treated with **11**, **12**, and **13** (10 μM) and fulvestrant (10 nM) for 48 hr. Western blot was performed to detect ERα protein levels.

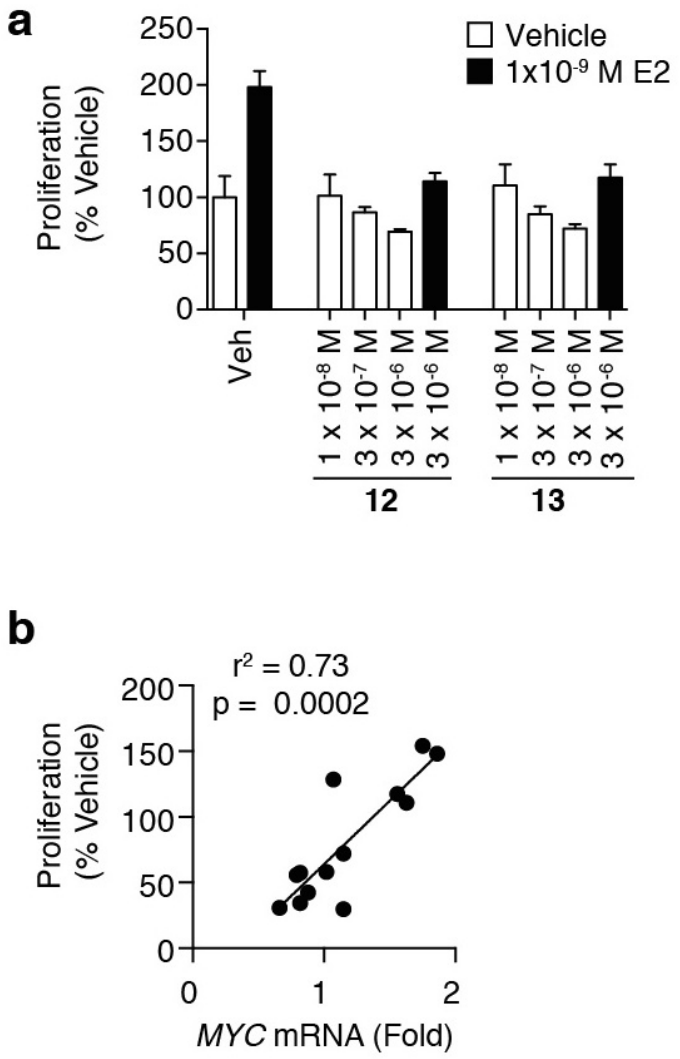

Supplementary Figure 6. ERα mediated control of proliferation

(**a**) Reversal of E2-mediated proliferation. MCF-7 cells (*n* = 4 biological replicates per group) were grown for 5 days in the presence of the indicated concentrations of **12** or **13** alone, or with vehicle (0.1% ethanol), or 10^{-9} M E2, or with 3 x 10^{-6} M of **12** or **13** together with 10^{-9} M E2. Values are mean ± s.e.m.

(**b**) Linear regression analysis for prediction of MCF-7 proliferation (from **Fig. 2a**) by *MYC* mRNA for compounds **1**–**13** (from **Fig. 3a**). Statistical significance was assessed with an F test for non-zero slope using GraphPad Prism software.

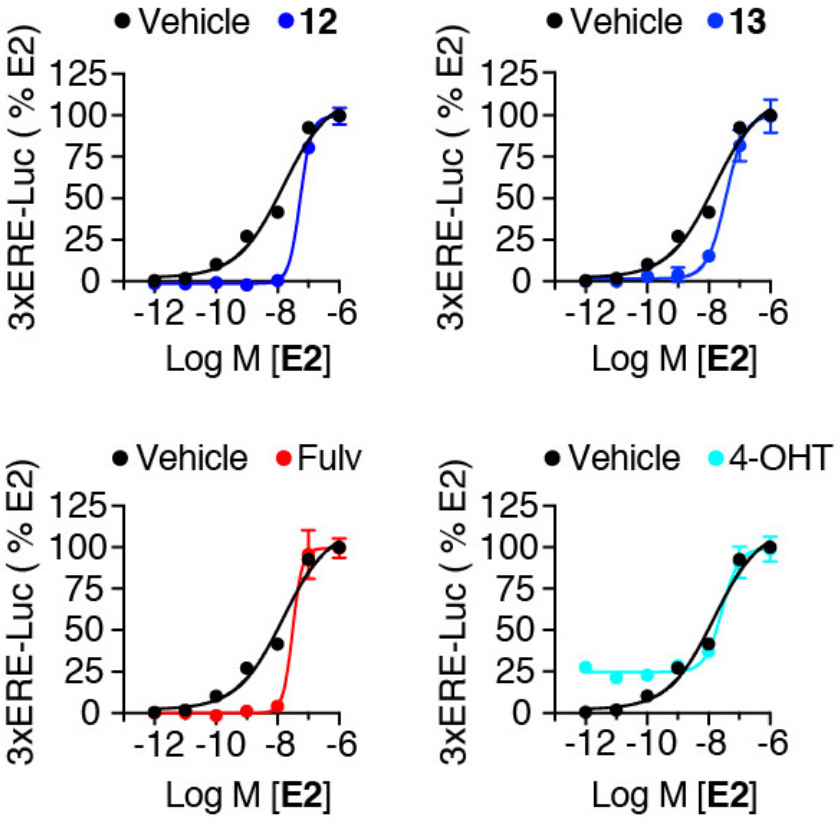

Supplementary Figure 7. Inhibition of ERα transcription by compounds 12 and 13 is fully reversed by E2.

HepG2 cells were transfected with 3xERE-luc and ERα expression plasmids. The next day, cells were treated for 24 hr with dose curves of E2 alone or in combination with compounds **12** (1 μM), **13** (1 μM), Fulvestrant (10 nM), or 4-OHT (10 nM). Data is shown as mean ± s.e.m. (*n* = 3).

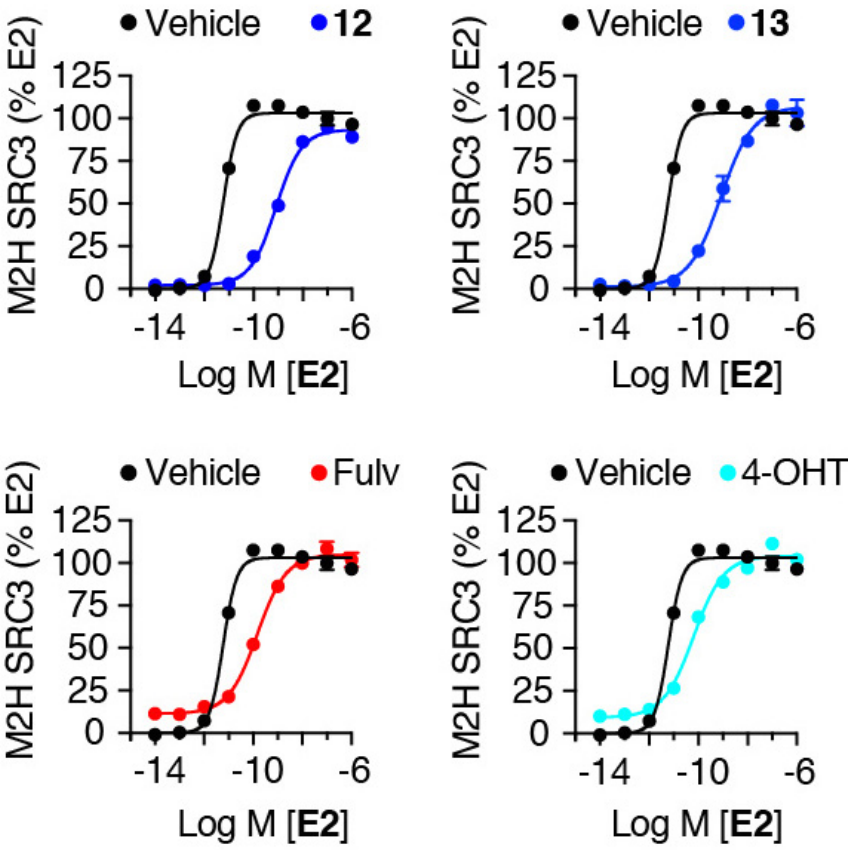

Supplementary Figure 8. Inhibition of ERα-SRC3 coactivator interaction by compounds 12 and 13 is fully reversed by E2.

HEK293T were transfected with VP16-ERα, GAL4-SRC3, and 5xUAS-luciferase plasmids. The next day, cells were treated for 24 hr with dose curves of E2 alone or co-treated with **12** (1 μM)**, 13** (1 μM), Fulvestrant (10 nM), or 4-OHT (10 nM). Data is shown as mean ± s.e.m. (n = 3)

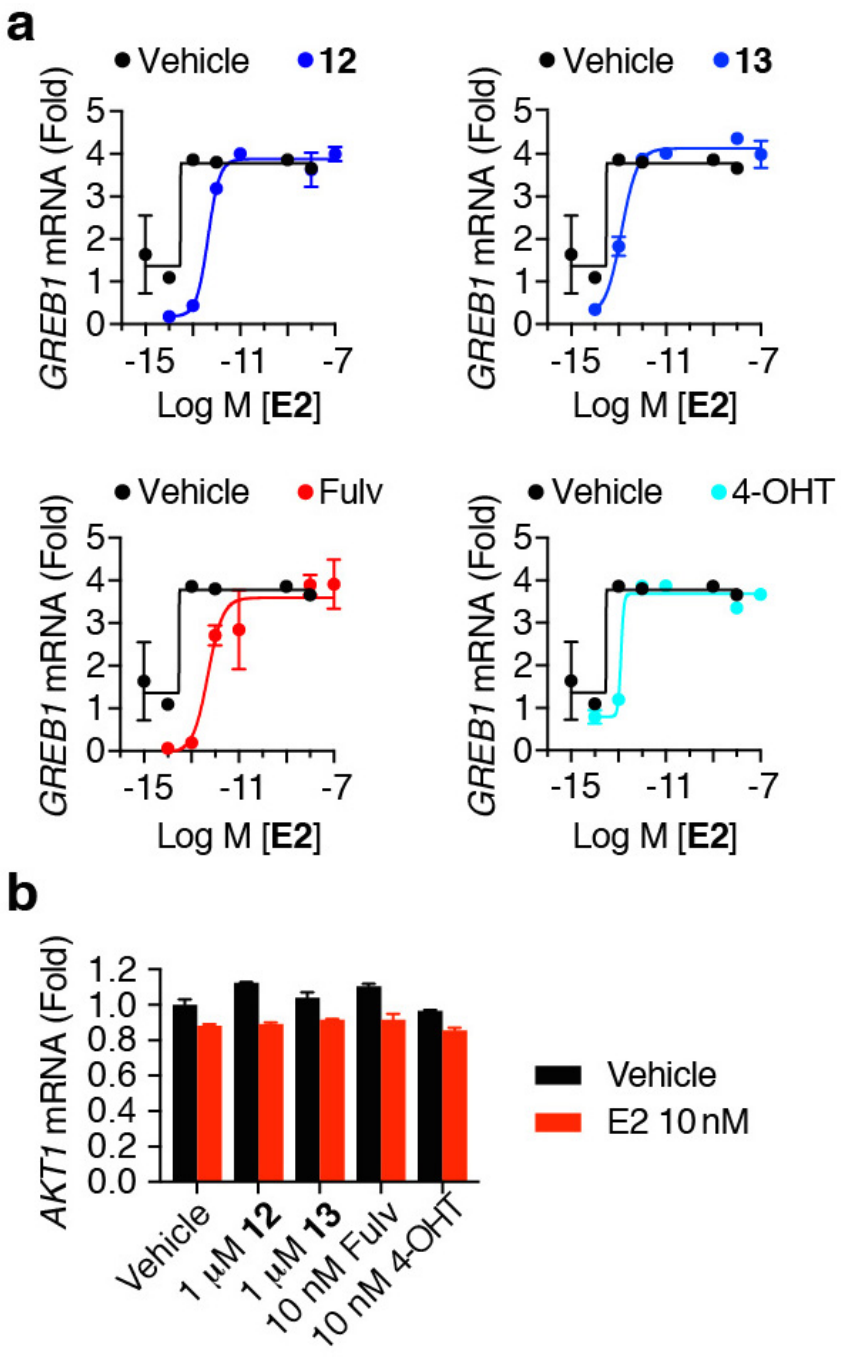

Supplementary Figure 9. Inhibition of *GREB1* mRNA by compounds 12 and 13 is fully reversed by E2.

(**a**–**b**) MCF-7 cells grown in steroid-free media were treated for 24 hr with dose curves of E2 alone or in combination with compounds **12** (1 μM)**, 13** (1 μM), Fulvestrant (10 nM), or 4-OHT (10 nM). $n = 2$ is shown as mean ± s.e.m. The mRNAs are normalized to *GAPDH*.

(**a**) *GREB1* mRNA.

(**b**) *AKT1* mRNA.

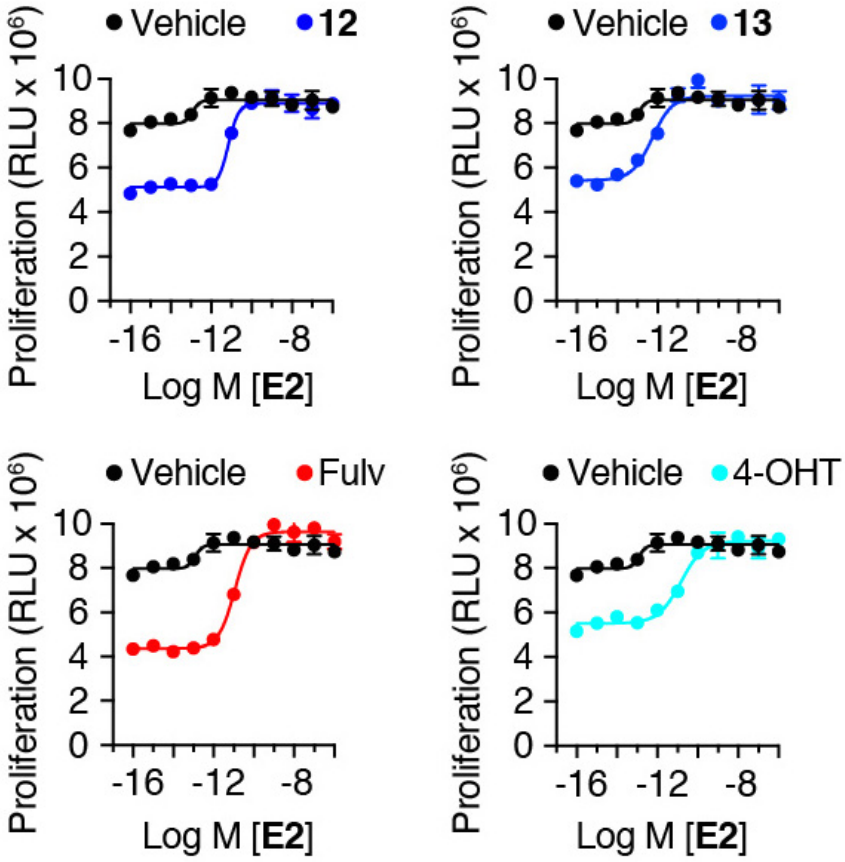

Supplementary Figure 10. Inhibition of MCF-7 proliferation by compounds 12 and 13 is fully reversed by E2.
MCF-7 cells grown in steroid-free media were treated for 5 days with dose curves of E2 alone or in combination with compounds **12** (1 μM)**, 13** (1 μM), Fulvestrant (10 nM), or 4-OHT (10 nM). Data is shown as mean ± s.e.m. (n = 3).

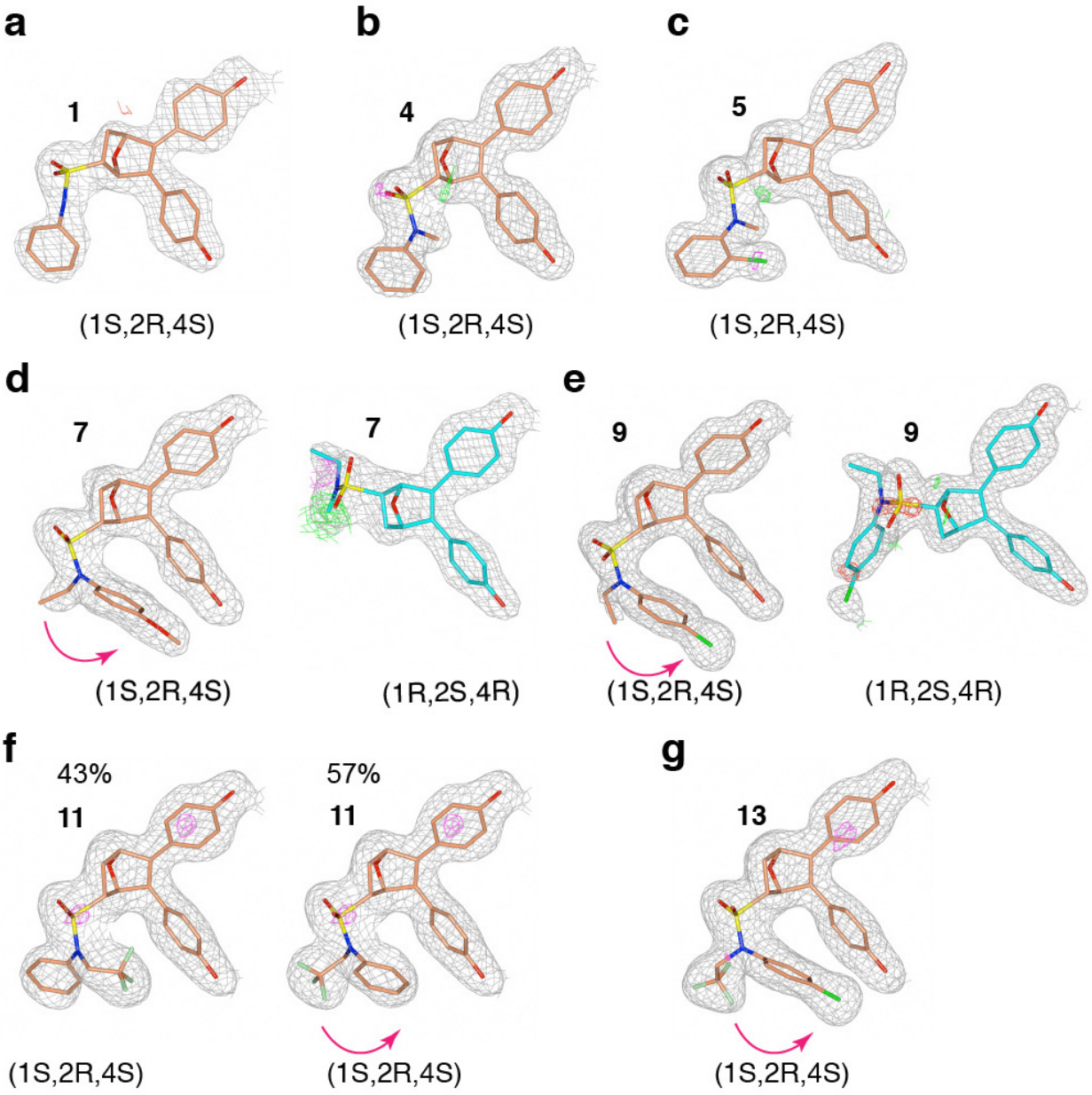

Supplementary Figure 11. Electron density maps of OBHS-N analogs inside the ERα ligand-binding pocket

(**a–g**) Each B chain subunit of the ERα LBD dimers contained the (1S,2R,4S) enantiomer (coral) of the OBHS-N analog. The $2F_o$ - F_c maps (grey) and the F_o - F_c difference maps (magenta and green) were contoured at 1σ and 3σ, respectively. Ligands were docked with COOT[5] and images rendered in CCP4MG[6]. (PDB 5KCC, 5KCD, 5KCE, 5KCF, 5KCT, 5KCW, 5KD9, respectively)

(**d–e**) The A chains of the **7**- or **9**-bound structures contained the (1R,2S,4R) enantiomer (cyan), while the A chains of the other structures contained the (1S,2R,4S) enantiomer (not shown).

(**f**) In the B chain, **11** displayed a mixture of binding orientations. Occupancy refinement in PHENIX software[7] was used to determine the relative percentages.

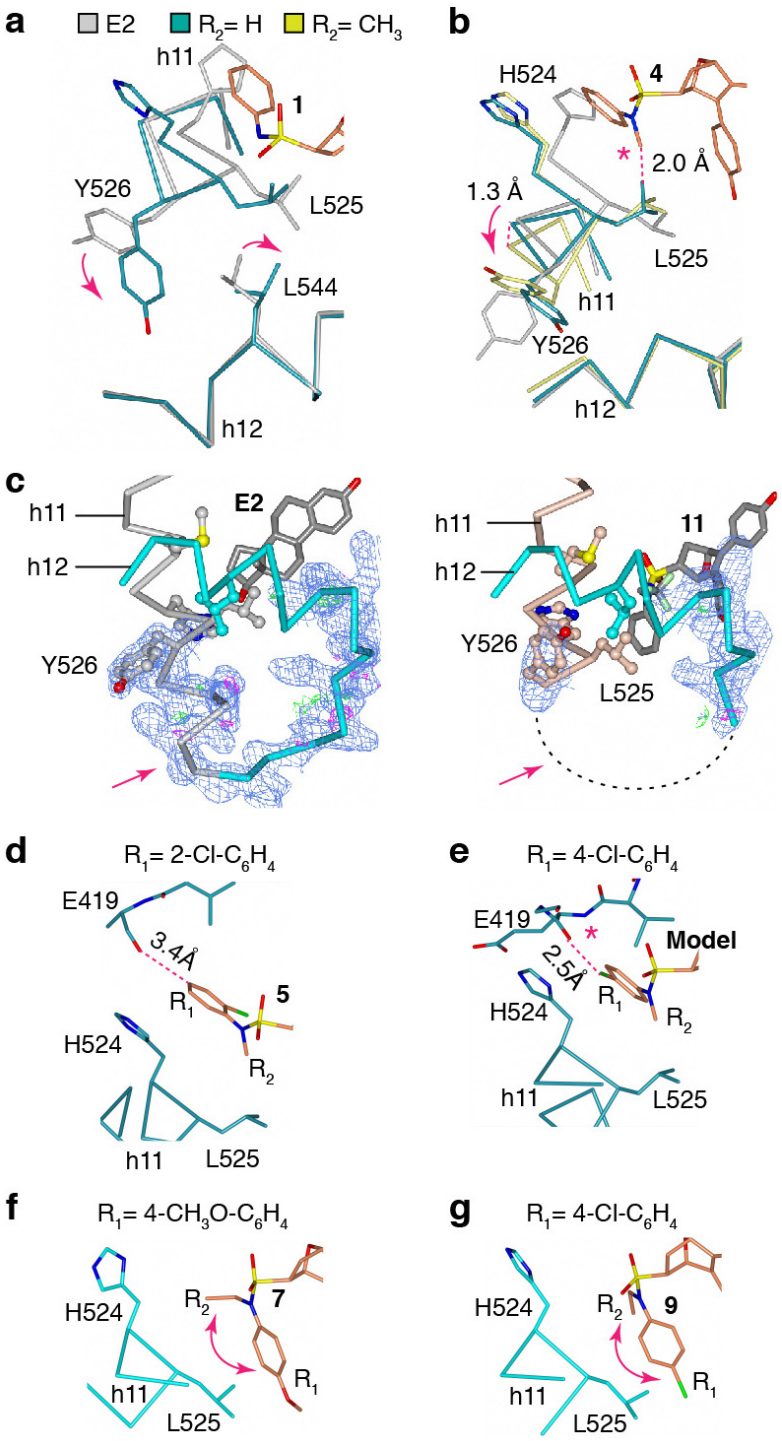

Supplementary Figure 12. Modulation of the h11–h12 interface by OBHS-N analogs

(**a**–**b**) Crystal structures were superposed to examine the effects of the OBHS-N R_1 groups on h11 positioning. **a**) The R_1 group of compound **1** displaced h11 from its E2-induced position and rotates the c-terminus of h11. **b**) In contrast to **1**, the methyl R_2 group of **4** rotates the h11 c-terminus in a different direction as is evident from the orientations of Tyr526. (PDB 3UUD, 5KCC, 5KCD)

(**c**) Electron density maps at the h11–h12 interface. The $2F_o$ - F_c maps (blue) and the F_o - F_c difference maps (magenta and green) were contoured at 1σ and 3σ, respectively. In compound **11**-bound structure, note the lack of electron density for the loop connecting h11 to h12. (PDB 3UUD, 5KCW)

(**d–g**) Orientations of the amide moiety of OBHS-N analogs with and without a *para*-substituted R_1 group. **d**) The OBHS-N R_1 groups are typically accommodated near His524, but **e**) modeling the *para*-substituted R_1 group in this orientation indicates a clash with the protein backbone at Glu419. **f–g**) Instead, the amide moiety is rotated to accommodate *para*-substituted R_1 groups near Leu525. (PDB 5KCE, 5KCF, 5KCT)

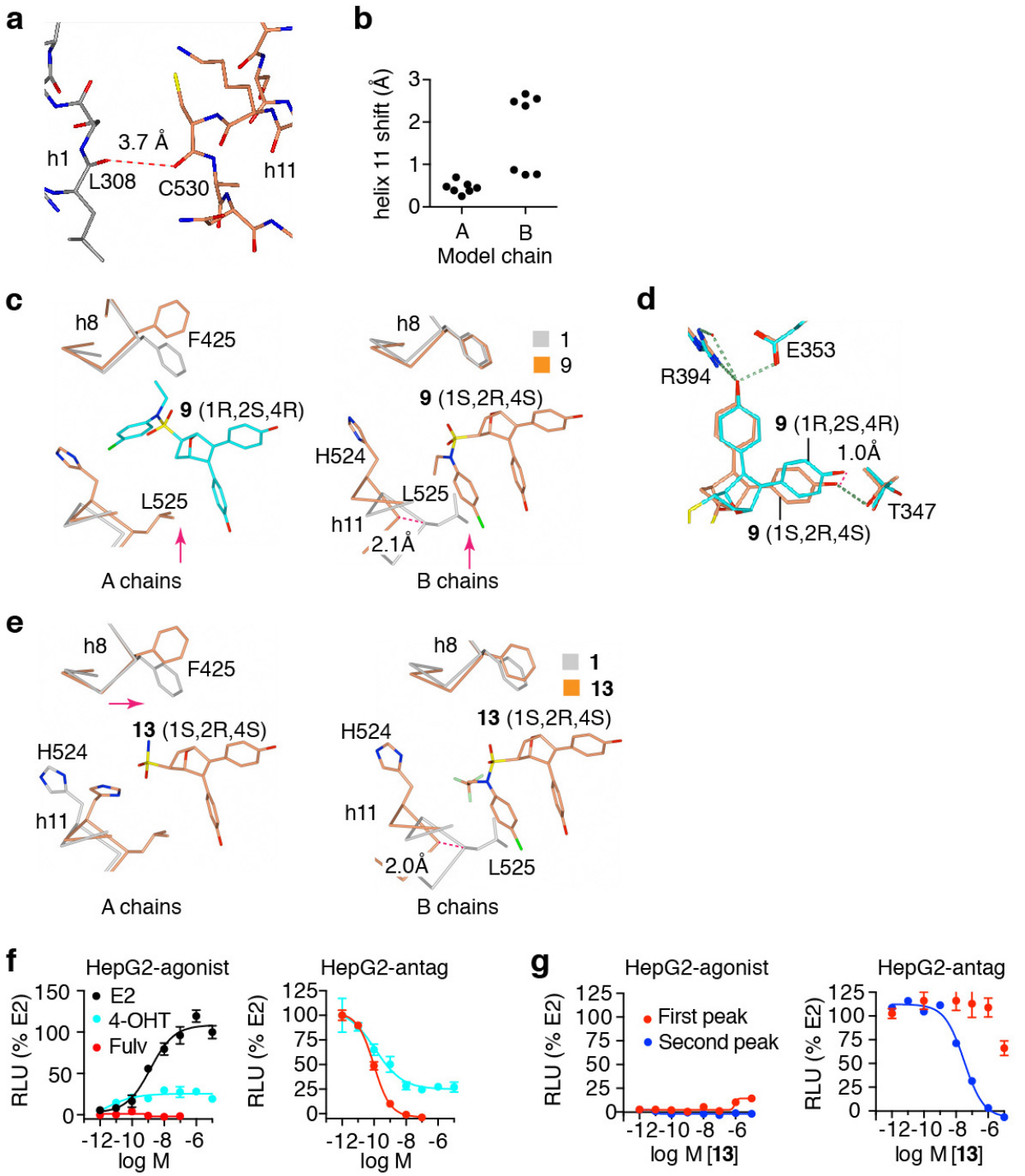

Supplementary Figure 13. Binding and activity of OBHS-N enantiomers.

(**a**) The backbone of helix 11 (h11) in the A chain of the dimer makes a close contact with the backbone of h1 in the symmetry-related molecule. (PDB 5KCT)

(**b**) Each of the OBHS-N structures was superimposed on the corresponding chain of the E2-bound ERα-Y537S structure (PDB 3UUD)[9]. The distance between the α-carbon of h11 Leu525 in the E2/ERα structure and the corresponding atom in each OBHS-N structure was measured.

Note that with respect to crystal packing, the A chain of the E2-bound structure corresponds to the B chain in the OBHS-N analog-bound structures.

(**c**) ERα structures bound to **1** and **9** were superimposed on the A or B chains. In the A chains the position of L525 prevents the shifting of the chlorophenyl towards the solvent (red arrow). (PDB 5KCC, 5KCT)

(**d**) The A and B chains of the **9**-bound ERα structure were superposed. In the A chain, the (1R,2S,4S) enantiomer phenol is 4 Å away from Thr347, while in the B chain the other enantiomer forms a 2.6 Å H-bond with Thr347. (PDB 5KCT)

(**e**) ERα structures bound to **1** and **13** were superimposed on the A or B chains as in (**c**), showing that the same enantiomer binds in both monomers, but with different orientations of the R groups. (PBD 5KCC, 5KD9)

(**f–g**) HepG2 cells were transfected with 3xERE-luc reporter and ERα expression plasmids. The next day, cells were treated for 24 hr with dose curves of OBHS-N compound **13** enantiomers (peak 1 and peak 2 of the HPLC separation), E2, fulvestrant, or 4-OHT. For the antagonist mode assay cells were co-treated with 10 nM E2 for the antagonist. Data is shown as mean ± s.e.m. (*n* = 3).

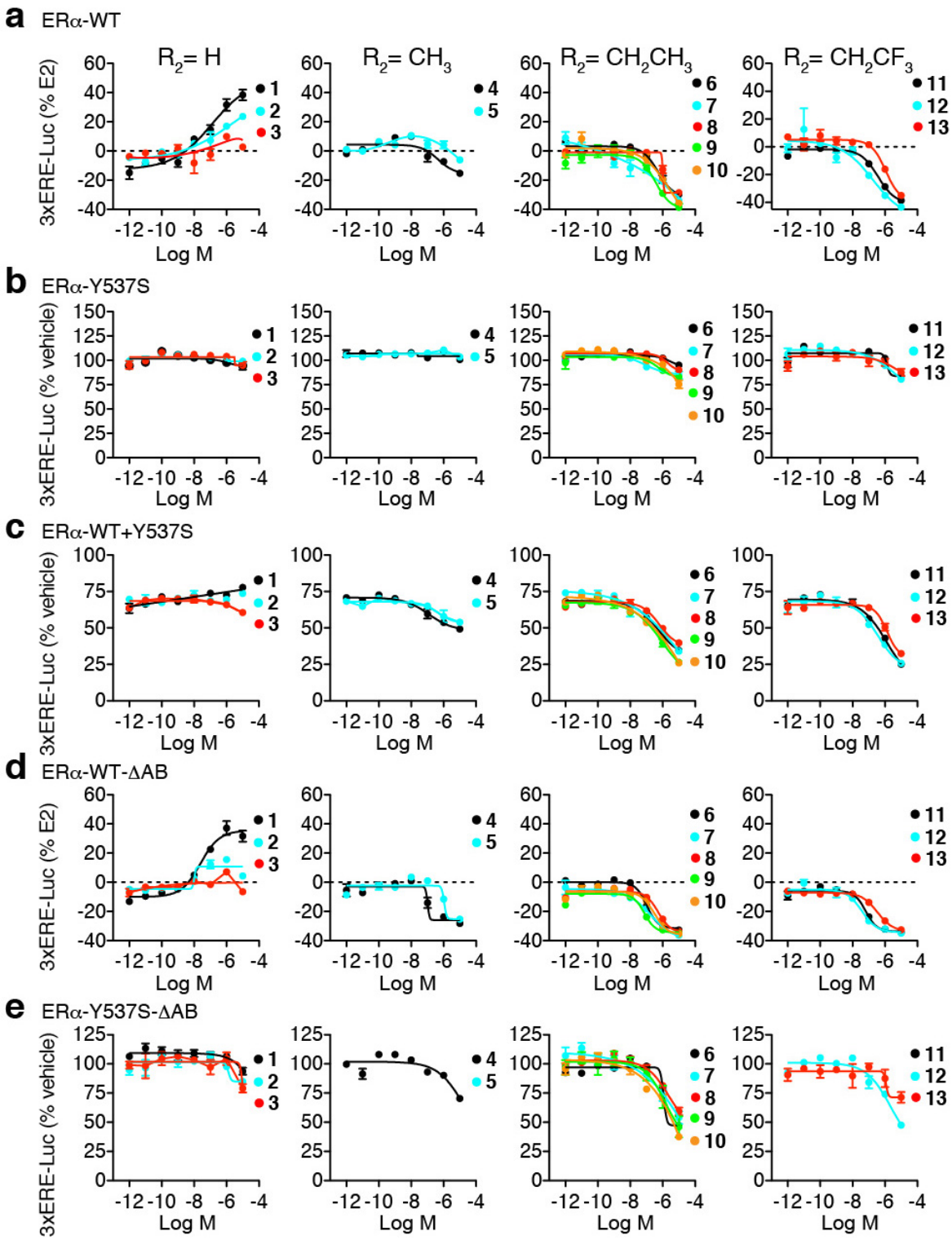

Supplementary Figure 14. Luciferase activity profiles with WT or mutant ERα

(**a–e**) 293T cells were transfected with 3xERE-luc and the indicated ERα expression plasmids. The next day, cells were treated for 24 hr with dose curves of indicated compounds. Data is shown as mean ± s.e.m. (n = 3).

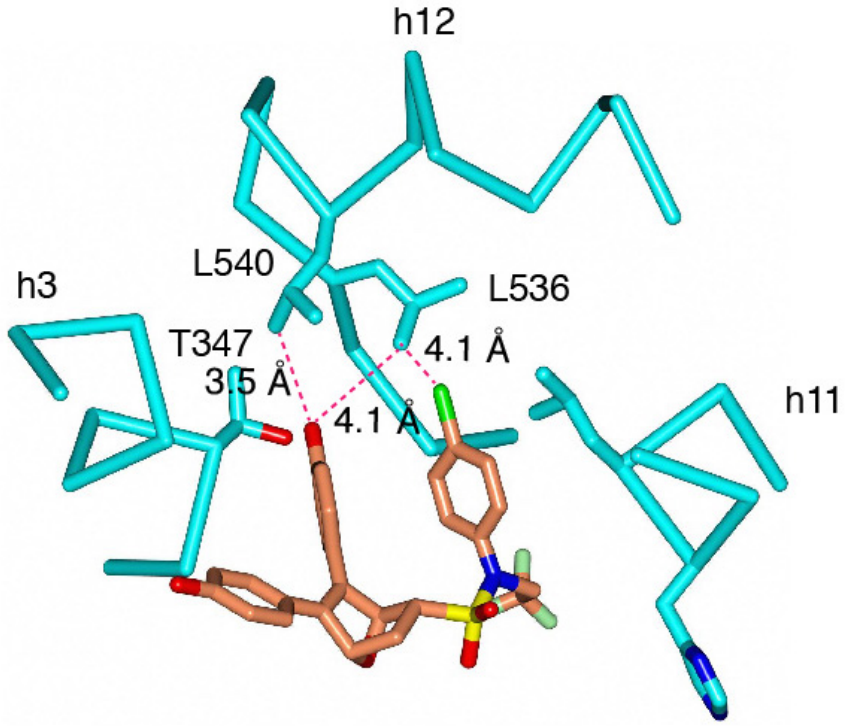

Supplementary Figure 15. OBHS-N compound has close contacts with the active conformer of ERα

Structure of the ERα-Y537S LBD bound to **13**. The indicated helices are shown as α-carbon traces (PDB 5KD9).

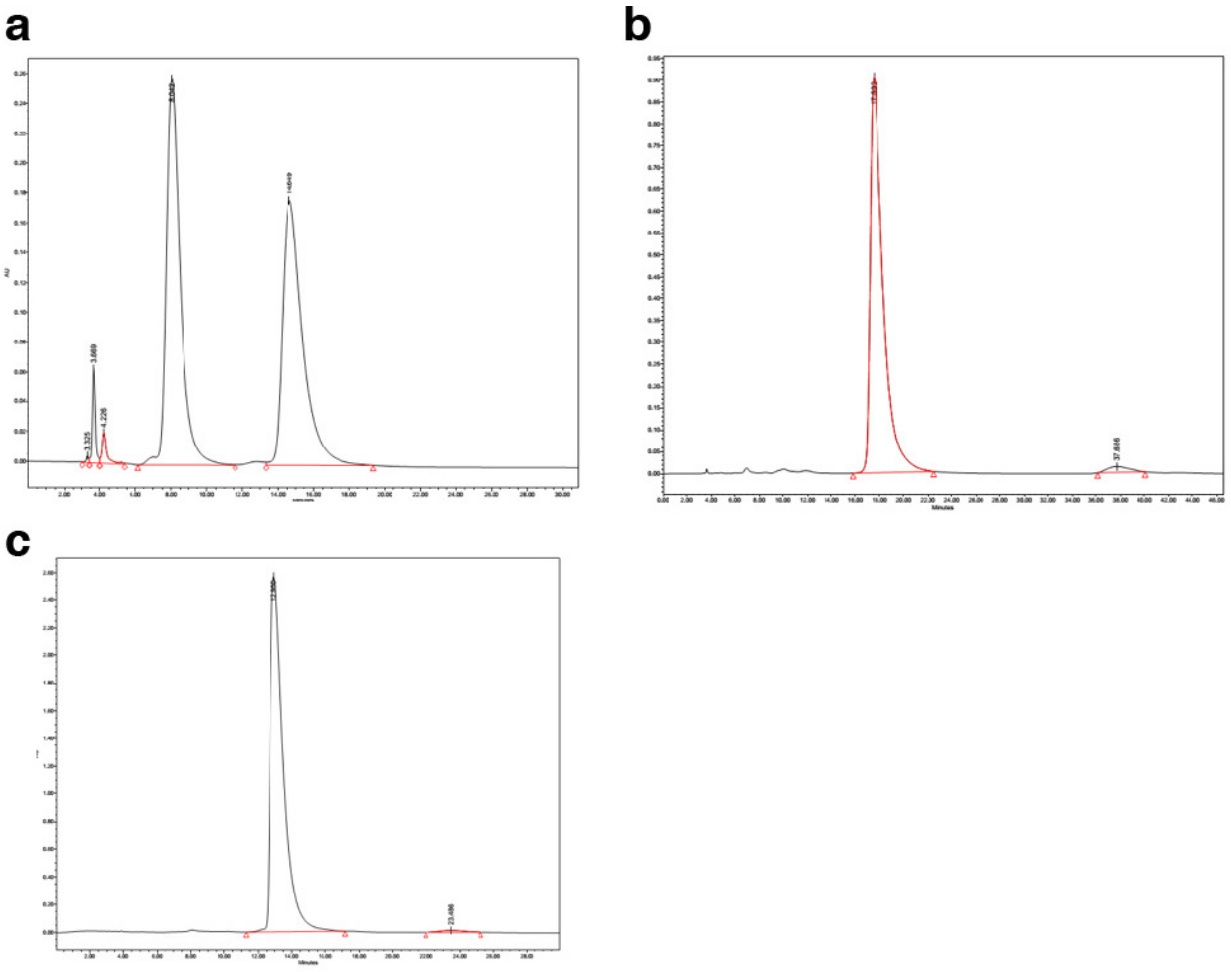

Supplementary Figure 16. HPLC separation of compound 13 entantiomers.

(a) Racemic compound 13 on Regis Tech Inc analytical (R,R) WHELK-O2 column. Mobile Phase: Hex: IPA = 50:50. Flow rate: 1 mL/min

(b) Purity test of compound 13 1st peak from Semi prep Column. Mobile Phase: Hex: IPA = 70:30. Flow rate: 1 mL/min

(c) Purity test of compound 13 2nd peak from Semi prep Column. Mobile Phase: Hex: IPA = 70:30. Flow rate: 1 mL/min

SUPPLEMENTARY REFERENCES

1. Shiau, A.K. et al. The structural basis of estrogen receptor/coactivator recognition and the antagonism of this interaction by tamoxifen. *Cell* **95**, 927-37 (1998).
2. Brzozowski, A.M. et al. Molecular basis of agonism and antagonism in the oestrogen receptor. *Nature* **389**, 753-8 (1997).
3. Wu, Y.L. et al. Structural basis for an unexpected mode of SERM-mediated ER antagonism. *Mol Cell* **18**, 413-24 (2005).
4. Pike, A.C. et al. Structural insights into the mode of action of a pure antiestrogen. *Structure* **9**, 145-53 (2001).
5. Debreczeni, J.E. & Emsley, P. Handling ligands with Coot. *Acta Crystallogr D Biol Crystallogr* **68**, 425-30 (2012).
6. McNicholas, S., Potterton, E., Wilson, K.S. & Noble, M.E. Presenting your structures: the CCP4mg molecular-graphics software. *Acta Crystallogr D Biol Crystallogr* **67**, 386-94 (2011).
7. Adams, P.D. et al. The Phenix software for automated determination of macromolecular structures. *Methods* **55**, 94-106 (2011).
8. Zhu, M. et al. Bicyclic core estrogens as full antagonists: synthesis, biological evaluation and structure-activity relationships of estrogen receptor ligands based on bridged oxabicyclic core arylsulfonamides. *Org Biomol Chem* **10**, 8692-700 (2012).
9. Delfosse, V. et al. Structural and mechanistic insights into bisphenols action provide guidelines for risk assessment and discovery of bisphenol A substitutes. *Proc Natl Acad Sci U S A* **109**, 14930-5 (2012).